

## Molecularly Imprinted Polymer Solid-Phase Extraction (MISPE) for the Determination of Dinitro-ortho-cresol (DNOC) and Its Risk Assessment in Tomatoes

Raden Tina Rosmalina<sup>1\*</sup>, Muhammad Bachri Amran<sup>2</sup>, Sri Priatni<sup>1</sup>, Bimastyaji Surya Ramadan<sup>3</sup>, Novi Fitria<sup>1</sup>

<sup>1</sup>Research Centre for Environmental and Clean Technology, National Research and Innovation Agency, Bandung, Indonesia

<sup>2</sup>Department of Chemistry, Bandung Institute of Technology, Indonesia

<sup>3</sup>Department of Environmental Engineering, Faculty of Engineering, Universitas Diponegoro, Indonesia

\*Corresponding author email: [finarosmalina@yahoo.com](mailto:finarosmalina@yahoo.com), [rade026@brin.go.id](mailto:rade026@brin.go.id)

Received May 20, 2022; Accepted December 14, 2022; Available online March 20, 2023

**ABSTRACT.** In this study, the molecularly imprinted polymer solid-phase extraction (MISPE) method for the determination of dinitro-ortho-cresol (DNOC) before HPLC (High-performance liquid chromatography) analysis was conducted. This study aims to analyze the sorption behavior and the potential use of molecularly imprinted polymers (MIP) for DNOC extraction. MIP was prepared using a combination of methacrylic acid as the functional monomer; ethylene glycol dimethacrylate as the crosslinker, benzoyl peroxide as the initiator, and acetonitrile as the porogen. The results showed that the optimum adsorption of the material was achieved at pH 5 for a contact time of 30 min with an adsorption capacity of 137 mg/g. The ideal eluent for desorption was a mixture of methanol and acetic acid with a ratio of 3:1. The calculations showed that the adsorption process followed the Sips adsorption isotherm model ( $n = 0.967$ ), which indicated adsorption on both homogeneous and monolayer surfaces. Reusability studies that were conducted via three consecutive adsorption-desorption cycles resulted in recovery values of 109.4%, 108.8%, and 101.1%. The concentration of DNOC obtained from tomato samples was 0.65 mg/kg with a recovery rate of 87.17%; this was within the tolerable range between 80% and 110%. Based on the high recovery and low LoQ, this method can be used to quantify DNOC quickly.

**Keywords:** Adsorption; DNOC; imprinted polymer; MIP; tomato

### INTRODUCTION

Dinitro-ortho-cresol (DNOC) is an integral component of larvicides, ovicides, and insecticides typically used for agriculture. This compound acts as a polymerization inhibitor and is an intermediate compound in several industrial chemical processes. DNOC is usually formulated as an emulsion concentrated in water or oil media (Pelfrene, 2000). Due to its toxicity to humans, which often causes nausea, stomach disorders, and anxiety attacks, identifying and analyzing its presence in food sources is critical importance (Samarth et al., 2015). There are two methods typically used for the preparation and extraction of DNOC from samples before high-performance liquid chromatography (HPLC), including liquid-liquid extraction (LLE) (Ferreira et al., 2012) and solid-phase extraction (SPE) methods (Gao et al., 2012). The SPE method is most likely used since it can extract the different types of pesticides compound. This method is advantageous since it minimizes exposure to hazardous substances and reduces the overall extraction time by cutting down on the number of organic solvents needed (López-

Lorente et al., 2022). Since traditional SPE adsorbents, such as silica, C-18, SAX, and SCX, have low specificity and selectivity, the application of SPE procedures is often combined with MIP as the adsorbent to improve selectivity, specificity, and recovery rates. This technique is known as molecularly imprinted SPE (MISPE) (Yi et al., 2013). However, determining a promising sorbent is essential for the SPE method since the extraction process needs high sensitivity and selectivity of a complex matrix (Wang et al., 2019).

Polymer-based nano sorbent (PBN) is considered a novel and emerging material for sample preparation. Concerning other nanomaterials, this material has many reactive end groups, branched structure, unique 3-D molecular configuration, and extensive internal and external surfaces, which make them strong capability as binding agents in the adsorption process of many organic compounds (Mahmood et al., 2019). Many PBNs can be found in the environmental application, including molecularly imprinted materials, carbon-based nano sorbents, magnetic nano sorbents, silica-based nano sorbents,

and fibers (Dwivedi et al., 2020). In this case, molecularly imprinted polymers (MIP) are widely used as sorbent materials for the pre-concentrating pollutant in environmental and food samples since this method offers some advantages, namely cheap, notably resistant to heat and pressure, highly reproducible without any loss in activity, easy to use, and relatively stable while maintaining high mechanical strength (Ashley et al., 2017). MIP is a polymeric material synthesized via co-polymerization of the print molecule. A target analyte (or analog) with a functional monomer is composed via covalent and non-covalent interactions with crosslinkers for the appropriate porogen solvent.

Most dinitrophenol (DNP)-pesticide extraction studies use DNP as the target compound. Lezamiz and Jonsson (2007) proposed a liquid membrane method enhanced by hollow fiber for determining four dinitrophenols in water samples (DNOC, DNP, Dinoseb, and Dinoterb). Other researchers evaluated DNP liquid extraction methods using different adsorbents such as modified silica (Wang et al., 2013), activated carbon (Krishnan et al., 2015), and molecularly imprinted polymer (Mehdinia et al., 2012). Quantitative analysis of DNOC and other dinitrophenol compounds also requires sample preparation techniques that isolate and concentrate the target analyte and eliminate matrix disturbances before measurements (Liu et al., 2013). The application of the novel MISPE for the extraction of organic compounds from food samples is quite interesting. However, a limited number of publications evaluate the application of the MISPE method for dinitrophenol compound analysis, especially DNOC as the targeted compound. Thus, the potential use of MISPE for DNOC extraction is still unknown since there is no available data presented in the published literature.

This research aims to synthesize and characterize a functional MIP through the MISPE method for the HPLC analysis of DNOC. MIP was prepared using methacrylic acid (MAA) as the functional monomer, ethylene glycol dimethacrylate (EGDMA) as the crosslinker, and benzoyl peroxide (BPO) as the initiator, and acetonitrile as the porogen. The

strength of the interaction between the mold molecule and the monomer was evaluated using UV-VIS spectrophotometry. This study used dried tomatoes samples from Cisarua, West Bandung District, Indonesia. Tomatoes are one type of fruit that is often consumed by Indonesian society because vitamin and mineral contents are very beneficial in increasing nutrition and health and are traded a lot at supermarkets and traditional markets in Indonesia.

## EXPERIMENTAL SECTION

### Chemical and Instrumentation

Fourier Transform Infra-Red (FTIR, Shimadzu IR Prestige-21), Spectrophotometer UV-VIS Agilent 8453, HPLC UV Agilent 1287 infinity, Thermal Gravimetric Analyzer (TGA, JEOL), and a Scanning Electron Microscope (SEM, JEOL-JSM-6510LV) were used for characterization analysis. Methanol, acetic acid, acetonitrile, MAA, EGDMA, and BPO were purchased from Merck. DNOC was purchased from Sigma-Aldrich. All other chemicals were analytical grade.

### MIP Synthesis

DNOC and MAA (1:1) were dissolved in acetonitrile by stirring for 1 hour before adding crosslinked EGDMA and the BPO initiator. The reaction mixture was shaken under N<sub>2</sub> gas for 10 min before heating at 70°C for 8 hours and was washed with methanol to remove excess reagents. The imprinted DNOC was extracted via soxhlation using a mixture of methanol/acetic acid (9:1) until it was no longer detectable with a UV-Vis spectrometer. Then, the resulting MIP mixture was repeatedly washed with methanol before drying at 80°C. NIP (non-imprinted polymer) and MIP polymer were characterized using FTIR spectroscopy (KBr pellets). Surface images of NIP and MIP were taken using SEM at a magnification of 5000 to determine the physical and chemical changes MIP had undergone due to the heating process. NIP and MIP were also characterized using TGA measurements conducted between 25°C and 500°C. Mass loss data at certain temperatures were obtained to calculate the first derivative curve for mass loss. The formation of MIP can be seen in **Figure 1**.

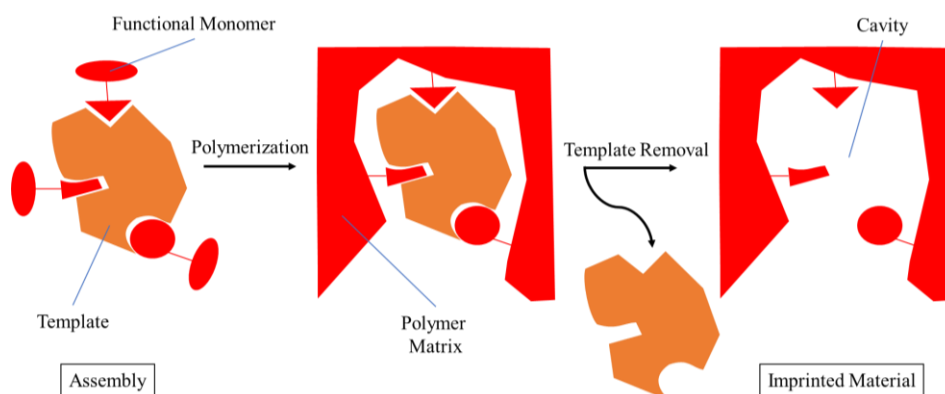


**Figure 1.** MIP Formation Principle

### Adsorption Test

The adsorption test was carried out by optimizing several parameters, including pH, contact time, and the effect of initial concentration under various conditions. The adsorption capacity of the polymer, which was the amount of MIP required to adsorb a given amount of DNOC, was calculated as equation [1]:

$$[S] = V \frac{C_0 - C_i}{mMIP} \quad [1]$$

Where:

- S = Amount of DNOCs bound in the MIP (mg/g)
- V = Volume of solution (L)
- Co = Initial concentration of DNOC (mg/L)
- Ci = Final concentration of DNOC after filtering (mg/L)
- m = Mass MIP used (g)

The resulting MIP was inserted into the SPE column and loaded with DNOC (100 ppm). During elution, the eluent composition was varied in a 9:1 and 3:1 ratio of methanol/acetic acid. The filtrate obtained was analyzed using a UV-Vis spectrophotometer. To establish the reusability of the sorbent, the SPE column filled with MIP was reloaded with DNOC (100 ppm). Elution was carried out using a mixture of methanol/acetic acid with a ratio of 3:1, and the eluate was measured using a UV-Vis spectrophotometer. The entire process was repeated for three cycles.

### Validation Method

The validation method includes tomato extraction and quantification by HPLC. The dried tomato samples were extracted with methanol. Only 5 g of tomatoes and 25 mL of methanol were used in this step. Next, MIP was used as d-SPE during clean-up for interferences removal. In this step, 100 mg of MIP was used to clean up 5 mL aliquots from the extraction. No evaporation that is usually used in pesticide analysis was involved in this method. The optimization of the d-SPE clean-up step was evaluated based on the recovery values and the precision of the triplicate samples. The recovery value of DNOC is in the range of 80 – 110%, as suggested by AOAC for residue analysis of pesticides. The method was validated for accuracy, linearity, precision, and limit of quantification (LoQ). For each spike concentration, the extraction was performed in triplicates. Accuracy was evaluated as percent recovery values while the average peak areas were plotted against the concentration as a calibration curve. Precision was calculated as percent relative standard deviation (RSD). LoQ was calculated using the signal-to-noise ratio (S/N) of > 3 (n = 3). Statistical analysis was performed in Microsoft Excel.

### Risk Assessment in Tomato Samples

The DNOC content in tomatoes was investigated due to the fruit's popularity in the Indonesian diet, and the fact shows that DNOC is commonly used as

a pesticide for tomato cultivation. Firstly, tomatoes were freeze-dried to remove the water content before being subjected to extraction for 24 h. Centrifugation was employed to separate the extracted solution for 5 minutes at 5,000 rpm. This was more effective than simple filtration because it did not result in DNOC residue on the filter paper. The supernatant was then placed in a 4-mL SPE column and was subjected to washing with water to remove any excess sample. The elution was conducted using 2 mL of methanol/acetic acid (3:1), and tomato samples were concentrated twice. Elution fractions were subjected to HPLC analysis on a C-18 column with methanol/water (45:55) as the eluent. The supernatant was then separated and loaded onto the SPE column before the elution with HPLC analysis of the eluate was conducted. For comparison, the DNOC content of another tomato sample solution was also directly measured using HPLC without prior application of the SPE process.

According to Sakthiselvi et al. (2020) soil ecological risk assessment was determined with Risk Quotient (RQ), which was calculated for earthworms (*Eisenia foetida*) and arthropods (*Aphidius colemani*, adult) with equation [2] (Tulcan et al., 2021):

$$RQ = \frac{EEC}{PNEC} \quad [2]$$

Where :

- RQ : Risk Quotient
- EC : The environment exposure concentration
- PNEC : The predicted no effect concentration

Levels of risk were classified into 5 risk levels: negligible ( $\leq 0.01$ ), low (0.01), medium (0.1), high (1), and very high risk ( $> 1$ ) (Sakthiselvi et al., 2020). In addition to providing risks to soil microorganisms, DNOC also provides a risk of water contamination through runoff during the rainy season (Mekenzie et al., 2020). In water, DNOC is present in the ionic form with a pKa value of around 4.3. Thus, if the presence of suspended organic matter increases in the water body, it will cause a longer time for degradation of DNOC in the aquatic ecosystem. It is known that the photocatalytic process to degrade DNOC occurs faster (50-90 minutes) in water media. However, the presence of organic matter can inhibit the photocatalytic process during the catalysis process when the transformation of nitrogen from DNOC to ammonia may occur (Arora et al., 2014). To determine the bioaccumulation factors (BAFs) DNOC in organic matter such as a river or marine biota, the ratio of the contaminant concentration in aquatic organism's tissue (Cr) to the contaminant concentration ratio in water (Cw), which includes uptake from all exposure routes, and if the BAF is > 5,000 L/kg in aquatic determined as equation [3] (Hilhor et al., 2019):

$$BAF = Cr/Cw \quad [3]$$

Where :

- BAF : Bioaccumulation (L/kg)

Cr : The ratio of the contaminant concentration in aquatic organism's tissue

Cw : The contaminant concentration ratio in water

Apart from being a risk to the environment, DNOC is also dangerous to human health if consumed. Exposure of DNOC compounds to humans happens through direct contact, digestion, and inhalation, but the potential exposure indirectly through the environment must be anticipated. Risk assessment due to human health is designed to calculate or estimate the risk for a particular target (Putri et al., 2021). According to the EPA, there are 4 basic steps for the human health risk assessment strategy, including hazard identification, dose-response assessment, exposure assessment, and risk characterization (US EPA, 2014). In the exposure assessment step, the exposure of tomatoes pesticides residues quantified for potential intake of pesticides residues is divided by the body weight and compared to Acceptable Daily Intake (ADI) values as determined in the dose-response assessment step as equation [4].

$$\text{Exposure} = \frac{\left\{ \text{Concentration of pesticides residues} \left( \frac{\text{mg}}{\text{kg}} \right) \times \text{food consumed} \left( \frac{\text{kg}}{\text{person day}} \right) \right\}}{\text{body weight (kg)}} \quad [4]$$

The risk characterization of applied pesticides mostly has non-carcinogenic effects. For non-cancer hazard calculation data used, hazard quotients for each pesticide (HQ<sub>i</sub>) and the hazard index (HI). The value of HQ<sub>i</sub> for children, adolescents, and an adult were assessed based on the ratio between estimated the corresponding ADI values and the estimated pesticides ADD as equation [5] (Hilhor et al., 2019):

$$HQ_i = \frac{ADD}{ADI} \quad [5]$$

Where :

ADD : Average daily intake

ADI : Acceptable daily intake

By ingestion of contaminated tomatoes, humans could be exposed DNOC with toxic effects; which have led us to consider identifying the cumulative hazard index (HI) using equation [6] (Hilhor et al., 2019):

$$HI = \sum_{i=1}^n HQ_i \quad [6]$$

Where :

HI : Hazard Index

HQ<sub>i</sub> : Hazard Quotients

HQ and HI of  $\leq 1$  are considered acceptable risk levels, and if  $\geq 1$  is regarded as a potential risk to exposed human health (Thi et al., 2021). Human health risk assessment due to contamination in agricultural regions is divided into two characteristics, the cancer risk assessment and hazard quotient (non-carcinogenic) assessment (Yusiasih et al., 2021). DNOC can be measured in the blood, urine, and tissue of exposed persons, and EPA includes DNOC as non-carcinogenic substance yet chronically exposed to residue in food (Jeong et al., 2012). To

considering ingestion the path of exposure and based on information provided (Hilhor et al., 2019) the Average Daily Dose (mg/kg/day) showed in equation [7]:

$$ADD = \frac{C \times IR \times EF \times ED}{BW \times AT} \quad [7]$$

Where :

C : The residue level (mg/kg)

IR : The ingestion rate or consumption rate of food group (g/day)

BW : The body weight (kg)

AT : The averaging time (year)

## RESULTS AND DISCUSSION

### Material Synthesis, Polymerization, and Characterization

The bulk method was employed to synthesize NIP and MIP in which MAA and EGDMA were used to generate the polymer structure of MIP. MAA interacted with the DNOC printing process through hydrogen bonds as a monomer, whereas EGDMA acted as a morphological controller for the polymer matrix. Polymer morphology was presented in the form of a gel, a macropore, or micro-powder particles. EGDMA also provided much-needed stability to the printed molecule matrix through its interaction with the binding site, which allowed for the generation of a high crosslink ratio. To this end, a crosslink mole ratio was achieved, which was four times greater than that of the functional monomer. Generally, oxygen is known to inhibit free-radical polymerization; thus, removing any dissolved oxygen from the solution is necessary to maximize the propagation rate and ensure reproducibility of the polymer (Supramono et al., 2019). Here, the removal of dissolved oxygen was carried out via ultra-sonication when the addition of the reagents during the experiment and after the addition of the initiator. BPO was used as an initiator since its radical formation mechanism was triggered via the heating process. Acetonitrile served as the solvent because of its volatility, which promoted a relatively shorter drying time for the polymer. Additionally, acetonitrile encouraged the formation of pores in a polymer and, thus, acted as the porogen in this case. The ability of MIP to selectively imprint molecules is influenced by the formation of complexes between the imprinted molecules and the monomers of interest. Imprinted molecules are critical in the molecular printing process because they direct the position of the functional monomers in the polymer matrix (Fu et al, 2015; Cheng et al., 2015). In our experiment, the hydroxyl group in DNOC, which acted as a hydrogen bond acceptor (base), prompted us to use MAA as a hydrogen bond donor counterpart.

The occurrence of leaching in the imprinted molecule was investigated via soxhlation in a solvent

mixture of methanol/acetic acid in a ratio of 9:1 at 80°C for 24 hours. This method produced more templates, which could trap DNOC in MIP since the solvent entering the Soxhlet extractor was not always saturated with DNOC. Therefore, the equilibrium reaction, which took place during extraction, always led to the release of DNOC from MIP. Additionally, soxhlation promoted better dissolution of the print molecule since extraction was carried out using a hot solvent, eliminating the need for an additional filtration step after extraction. Given this, it can be said that leaching of the print molecule is an essential step in the MIP synthesis process as the presence of leftover print molecules in the MIP complex reduces the number of binding cavities available for the target molecule.

Characterization results from FTIR spectroscopy have been published elsewhere (Rosmalina et al., 2019). The existence of a C=O carbonyl ester is derived from cross-polymerization between MAA and EGDMA. Similarly, a C–O stretching vibration is observed at 1259.52  $\text{cm}^{-1}$  in all three spectra. At a magnification of 5000, NIP and MIP are seen to have very different porosity and surfaces. The surface of NIP is homogeneous and smooth, whereas MIP–DNOC is more heterogeneous and rougher. After leaching, the surface of MIP becomes homogenous, while MIP that has been reattached to the DNOC imprinted molecule is coarser and much more heterogeneous. The loss of the DNOC molecular imprint is at around 290°C, which corresponds to the decomposition temperature of DNOC at 312°C. In the second incident, the shift in the temperature of the mass loss from 417°C for NIP to 424°C for MIP indicates the presence of other compounds in the MIP matrix. Overall, MIP experienced more significant mass loss (90.75%) than NIP (89.73%).

### Validation Result

DNOC peak was observed in the spiked sample (Figure 2), suggesting that the method was able to extract DNOC from the tomato's matrix. DNOC analysis is critical due to its use as selective herbicides in agriculture practices such as grain, hops, vegetables, and fruits. Apart from being used as an herbicide, DNOC is often used as a larvicide and inhibitor of the polymerization process in the plastics, dyeing, and pharmaceutical industries, the widespread use of DNOC could emerge as a potential risk to the quality of soil, water, and human health (Arora et al., 2014). The retention times for the DNOC standard and the tomato samples were 3.64 and 3.56 min, respectively. Confirmation tests were conducted to ensure that the peaks in the tomato samples were due to the presence of DNOC and not from other compounds that had identical physical and chemical properties. This study was carried out by spiking technique in which standard concentrations of DNOC were added to the tomato samples before analysis. Ideally, the resulting peak should show the same retention time and a markedly increased peak area compared with the chromatograms for pure DNOC (Figure 2). Conversely, if there is no change in the peak area and the sudden appearance of two peaks, then it is safe to say that the compound in question is not DNOC. One key advantage of the SPE method is carrying out pre-concentration procedures to eliminate the effects of the sample matrix and purify the sample further. Figure 3 shows that the tomato samples directly to HPLC analysis without SPE column treatment have a very complex sample matrix. On the contrary, the samples treated by the SPE column before HPLC analysis had a cleaner profile, and the only visible peak was due to DNOC.

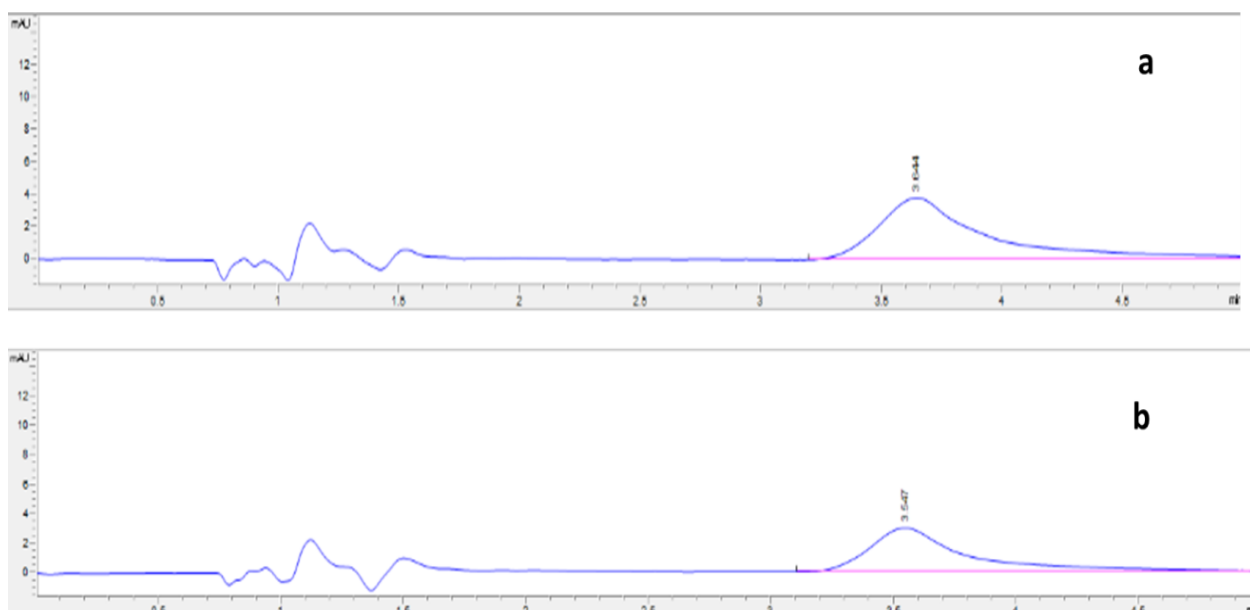
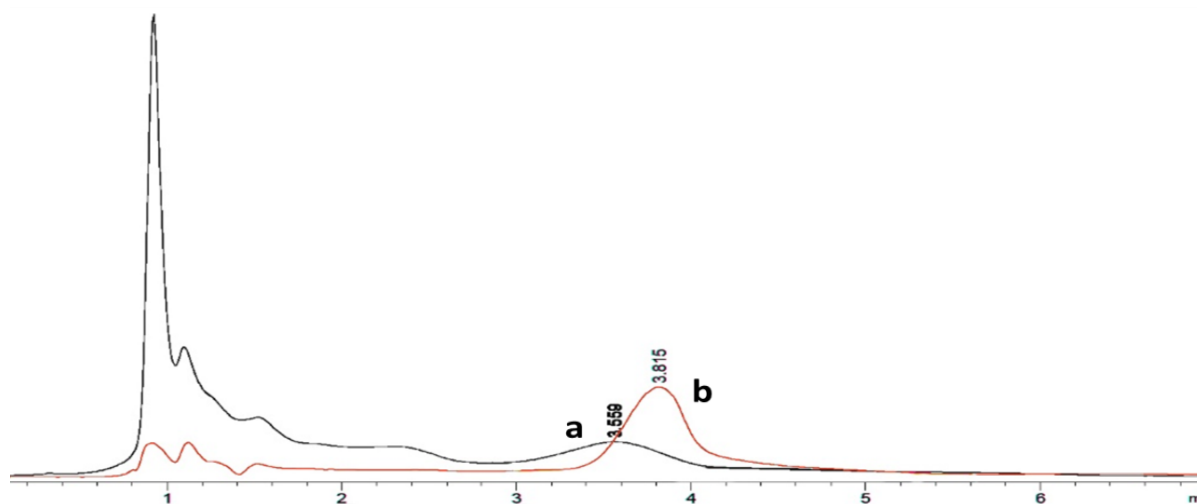


Figure 2. Chromatogram of (a) standard solution, (b) tomatoes samples.



**Figure 3.** Chromatogram of (a) tomatoes sample without SPE, (b) spiked sample by SPE

**Table 1.** Evaluation of the method

Compound	Precision $\pm$ % RSD <sup>a</sup>	% Rec <sup>a</sup> $\pm$ SD	Linear regression (R)	LoQ <sup>a</sup> (mg/kg)
DNOC	0.66 $\pm$ 1.85	87.18 $\pm$ 0.59	$y = 40.819x + 22.56$ (0.9993)	0.54 $\pm$ 0.87

<sup>a</sup>Results are the mean of five replicates  $\pm$  SD

Recovery values for the spiking experiment at 2.5 mg/kg and other method evaluation data are in **Table 1**. The percent recovery values for DNOC at a concentration of 2.5 mg/kg is in the range suggested by AOAC, which is 80 – 110%; thus, the recovery of this method is acceptable in this concentration. The calibration curve provided linear results in the concentration range of 2.5 to 15  $\mu\text{g/mL}$  with a correlation coefficient of 0.9993. This result suggests that based on the linearity, the method is acceptable. As seen in Table 3, the % RSD value for concentration is below the recommended value from AOAC, which is  $\leq 8\%$ . Therefore, the repeatability of this method is acceptable for 0.66 mg/kg. The correlation coefficient and the detection limits for dried tomatoes are presented in **Table 1**. The LoQ was 0.54 mg/kg, which is comparable to the LoQ of other analysis methods that utilize a periodate spectrophotometric method. Up to now, there are no MRLs of DNOC that have been regulated for tomatoes. Thus, the LoQ obtained in this study was compared to other methods. The LoQ of this method was 0.54 mg/kg, which is below the previous survey. Thus, this method is applicable for the quantification of DNOC in tomatoes.

#### Adsorption Test Result

The prevailing pH of the reaction solution exerts significant influence on the adsorption process, particularly related to the active groups on the surface of MIP and the solubility of DNOC. At pH values of 3 and 4, excess  $\text{H}^+$  in the solution from the water source encourages the formation of hydrogen bonds with the OH functional groups on DNOC and

MAA. Thus, the interaction between the DNOC print molecule and the MAA monomer is decreased, resulting in a relatively small adsorbed mass (**Figure 4a**). However, this trend is reversed when the pH of the solution is increased to the optimal level at pH 5. This condition is due to the heterogeneity of the reaction system since DNOC exists as a solution, whereas MIP-DNOC is solid. The optimum adsorbed mass observed at pH 5 is above the pKa for DNOC at 4.46. When the system's pH is higher than 5, the OH group in DNOC and COOH in the ionized monomer becomes increasingly negative, thereby discouraging the formation of hydrogen bonds and ultimately resulting in a lower adsorbed mass. The contact time is defined as the time needed for the DNOC adsorption reaction to reach equilibrium. When the adsorbed mass value is plotted against the contact time, a graph like **Figure 4b** emerges.

In this case, the adsorbed mass in MIP is shown to increase with a longer adsorption time of up to 30 min. This situation is because a more extended reaction increases the chance of interaction between the adsorbate molecule and the surface of MIP. However, it is essential to note that any additional time beyond the 30-min point does not provide any significant advantage for the polymer's adsorbed mass. This condition is because the surface of MIP is saturated with adsorbed DNOC and is, thus, unable to accommodate any more adsorbate. Conversely, the adsorbed mass of NIP reaches its pinnacle at the 90-min mark, indicating that the adsorption kinetics for NIP require a much longer time than that for MIP.

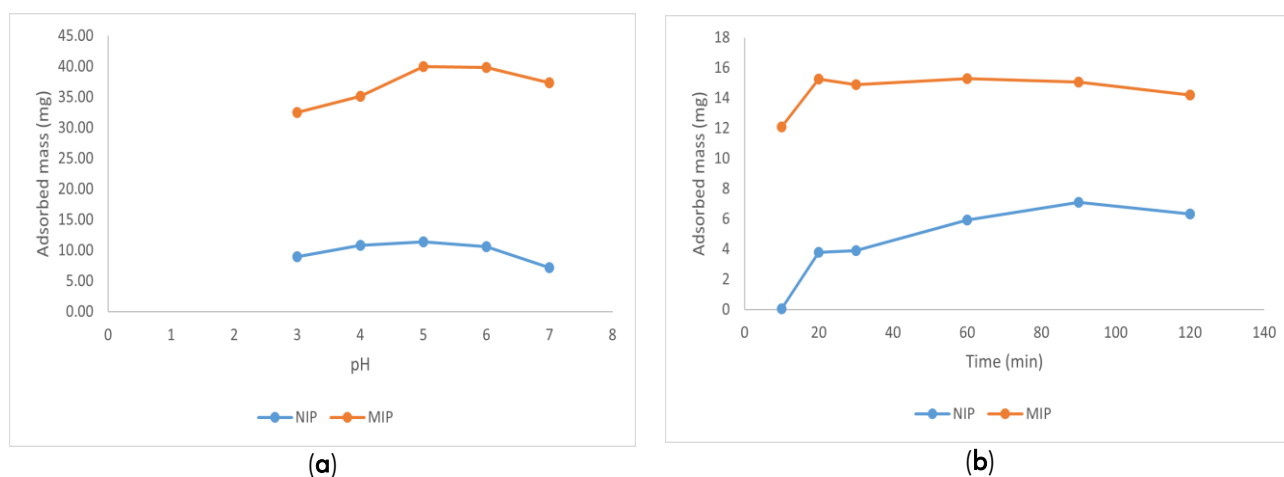


Figure 4. Effects of pH (a) and contact time (b) on adsorbed mass

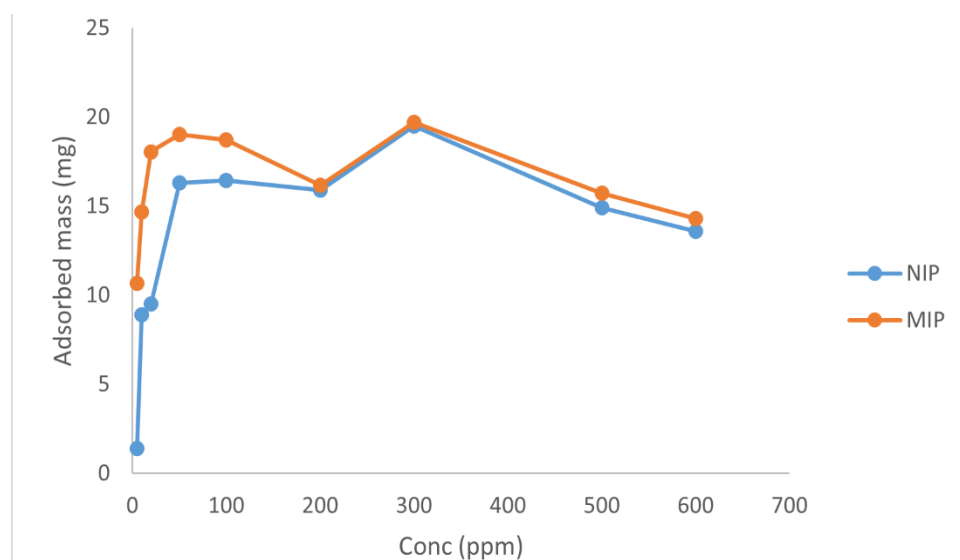


Figure 5. Effects of initial concentration on adsorption capacity

Table 2. Correlation coefficients and DNOC adsorption kinetics

Pseudo first order			Pseudo second order		
$K_1$ ( $\text{min}^{-1}$ )	$q_e$ (mg/g)	$R^2$	$K_1$ ( $\text{min}^{-1}$ )	$q_e$ (mg/g)	$R^2$
0.260	6.634	0.850	0.179	2.537	0.998

In Figure 5, the adsorbed mass is plotted against the initial concentration of DNOC. Here, MIP has a higher adsorbed mass for DNOC adsorption than NIP. This results from increased analyte adsorption through the addition of print molecules, i.e., higher DNOC concentrations allow for more interactions between DNOC and MIP. Figure 5 shows that the adsorbed mass increases significantly over a concentration range from 5 to 300 ppm. Beyond this point, however, the rate of the increase is only gradual, and although MIP is still able to adsorb DNOC, this is achieved with a capacity value of 137 mg/g at an initial concentration of 600 mg/L.

Pseudo-first order and pseudo-second-order reaction kinetics can be used to describe the

adsorption of DNOC onto the surface of MIP. The data needed to generate the DNOC adsorption kinetics in this study is obtained from the plot of DNOC adsorption values. For the second-order kinetics model, the correlation coefficient,  $R^2$ , is 0.998, whereas the first-order kinetics model has a correlation coefficient of 0.850, indicating that the adsorption kinetics of the reaction strictly follows the proposed models (see Table 2). Here, the pseudo-second-order kinetics model assumes that adsorption of DNOC by MIP occurs in two stages: when the adsorbate interacts with the surface of the adsorbent and when the adsorbate interacts with the adsorbate (Singh et al., 2014).

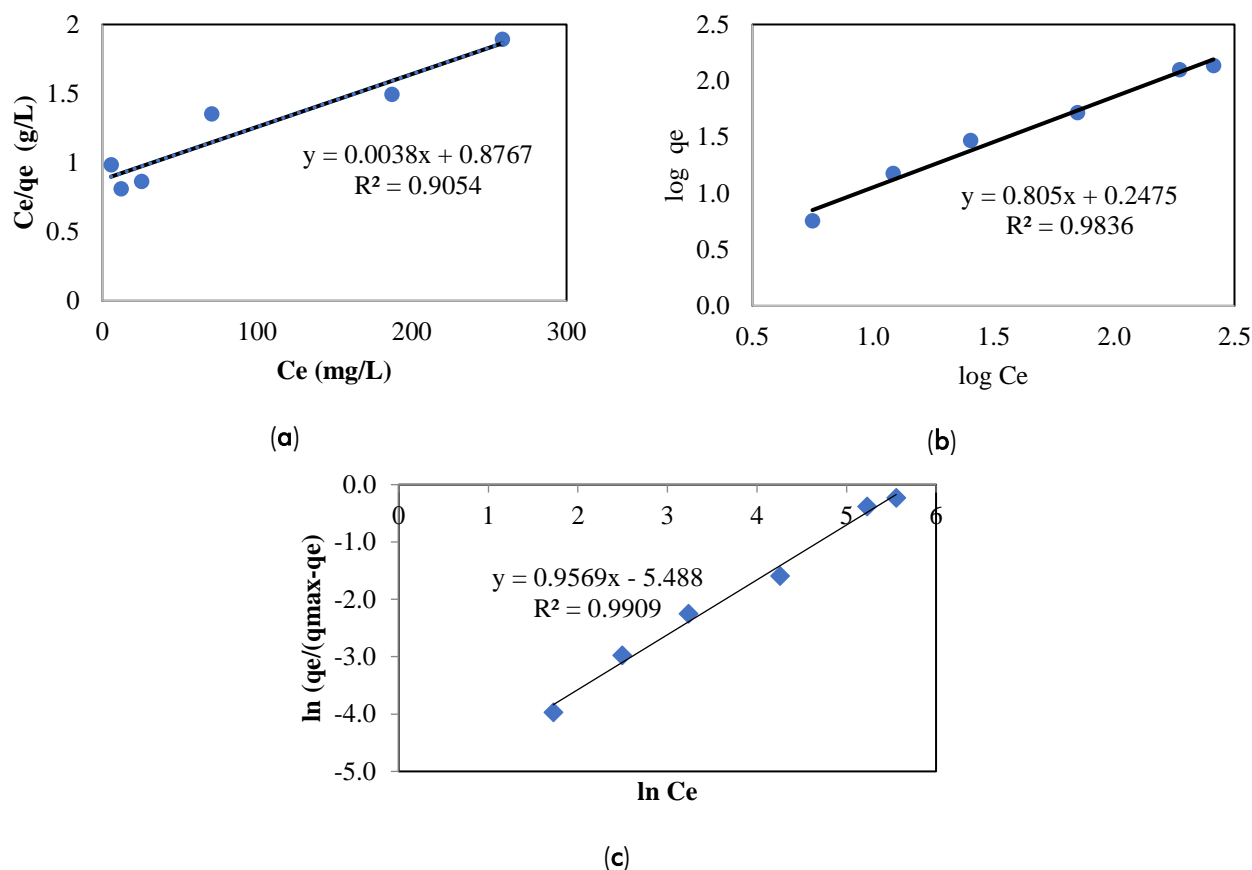


**Figure 6.** Model for DNOC adsorption by MIP–DNOC: **a.** Langmuir isotherm model; **b.** Freundlich isotherm model; **c.** Sips model

It is also essential to determine the adsorption isotherm to understand how adsorption occurs. Langmuir, Freundlich, and Sips models can be used since each model provides invaluable insight into the adsorption principles governing MIP and NIP. According to the Langmuir adsorption model, adsorption of a printed molecule only occurs on a monolayer surface, and the rate of adsorption does not depend on the number of molecules adsorbed (Abouelella et al., 2018). In this case, the model assumes that all sides of the adsorbent have the same affinity for the printed molecule; thus, adsorption on one side of the polymer does not affect the other side. Conversely, the Freundlich approach looks at heterogeneity on the surface and seeks to explain the relationship between the concentration of the analyte adsorbed and the concentration that is still in the surrounding solution.

The isotherm curves models of Langmuir and Freundlich are shown in **Figure 6a** and **6b**. The Langmuir isotherm curve model is obtained by plotting  $C_e$  against  $C_e/q_e$ , whereas the Freundlich

isotherm curve model is obtained by plotting  $C_e$  against  $\ln q_e$ . Based on the curve in **Figure 6a**, the correlation coefficient  $R^2$  of the Langmuir isotherm model is 0.9054. This analysis assumes that adsorption occurs on the monolayer (Rahman et al., 2018). In other words, since no more layers are formed once the monolayer is established, the surface of the adsorbent reaches a saturation point, and the maximum adsorption capacity on the surface of the adsorbent is achieved (Yahya et al., 2021). For the Freundlich model, the isotherm constant ( $K_f$ ) is calculated from the slope and is an intercept of the slope obtained from the plot of  $\ln C_e$  against  $\ln q_e$ . In this case, the affinity or interaction between MIP and DNOC template molecules is exemplified by the intensity of adsorption,  $n$ . A value of  $1 < n < 10$  illustrates that adsorption is preferred. Since the  $n$  value of Freundlich isotherm is 1.24, it is safe to say that the adsorption is preferred in this case. Based on the slope in **Figure 6b**, the correlation coefficient  $R^2$  of the Freundlich isotherm model is 0.9836.

**Table 3.** Parameters for Freundlich, Langmuir and Sips models

Freundlich			Langmuir			Sips		
N	$K_f$	$R^2$	$q_m$ (mg/g)	$R_L$	$R^2$	$K_{eq}$	N	$R^2$
1.2442	1.7681	0.9836	215.35	0.979	0.9054	0.0039	0.967	0.991

**Table 3** shows the  $R_L$  factors for the Langmuir isotherm, which can be used to predict the affinity between MIP and DNOC printed molecules. In this study, the  $R_L$  values of various DNOC concentrations tend to spread between 0.27 and 0.97, thereby supporting the notion that the adsorption process is preferred. Based on literature reports, the adsorption process is not preferred when the value of  $R_L$  exceeds 1, and it is linear when  $R_L = 1$ . If the value is  $0 < R_L < 1$ , then the adsorption process is preferred. When  $R_L = 0$ , the adsorption is irreversible (Chen et al., 2015). **Figure 6c** shows that at an initial concentration below 300 ppm, MIP–DNOC follows the Freundlich adsorption isotherm model. However, above this concentration threshold, the adsorption capacity of MIP–DNOC does not increase significantly and even tends to follow the Langmuir adsorption isotherm model. Based on this information, it can be concluded

that adsorption in our study is the product of a combination of the Langmuir and Freundlich adsorption isotherms, a model which is commonly referred to as the Sips adsorption isotherm. In this situation, the adsorption model approaches the classical Freundlich equation when the DNOC concentration is low but veers towards the Langmuir equation when the DNOC concentration is high due to analyte saturation. At a value of 0.991, the correlation coefficient  $R^2$  in our case closely approaches the ideal, which is additional proof that the DNOC adsorption process in this study adheres to the Sips adsorption isotherm model. Another aspect that was closely monitored in our study was the composition of the eluents used during SPE. With optimization in mind, desorption–adsorption studies were carried out using eluent compositions of methanol/acetic acid in the ratios of 9:1 and 3:1.

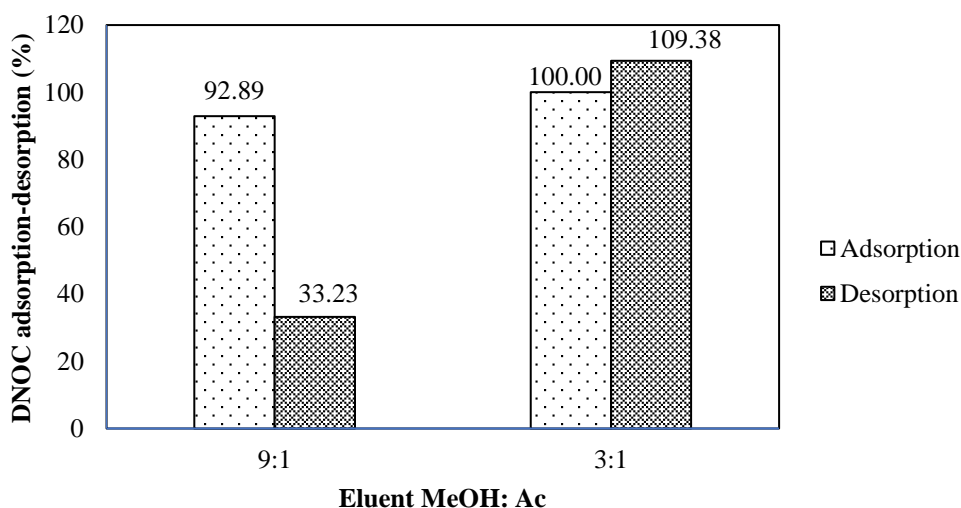


**Figure 7.** Comparison of DNOC desorption and adsorption percentages

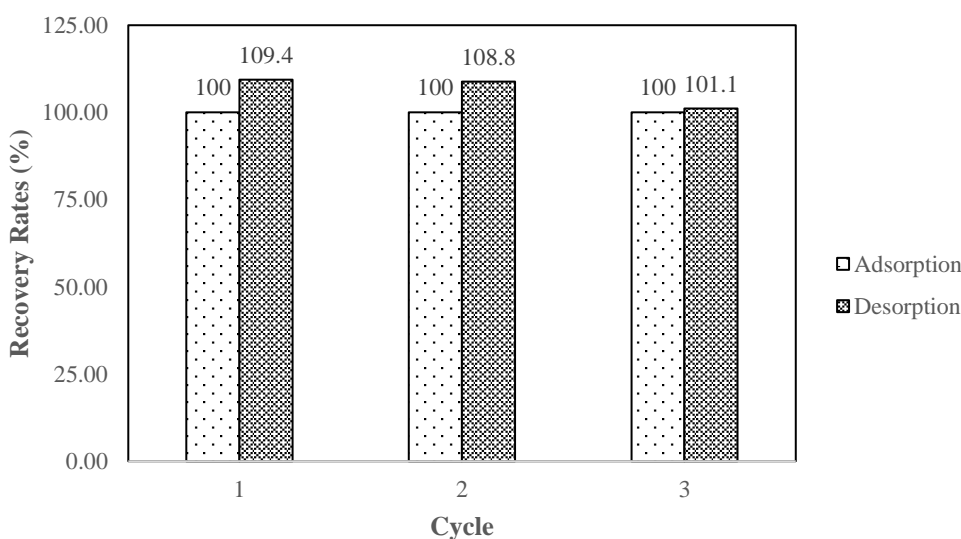


**Figure 8.** Comparison of MIP reusability

Based on **Figure 7** results, a mixture of methanol/acetic acid in a ratio of 9:1 allows for 33.23% DNOC adsorption-desorption, which means that this eluent mixture is simply not polar enough to elute DNOC from the MIP solid phase. Thus, a more polar eluent composition is tested (3:1 ratio of methanol/acetic acid) in which the percentage of acetic acid in the eluent is increased. Elution using this mixture results in 101.11% DNOC adsorption-desorption. The importance of reusability in these types of polymers cannot be overstated. Reusability studies are conducted on MIP-DNOC in which adsorption-desorption cycles are carried out thrice. As shown in **Figure 8**, MIP-DNOC is still quite effective at adsorbing DNOC even after three cycles, resulting in recovery rates of 109.4%, 108.8%, and 101.1%.

### DNOC Risk Assessment

Tomato is a nutritional product of agriculture with main antioxidant, anti-inflammatory, and anticancer activities, including DNOC residue that affects the environment and human health (Salehi et al., 2019). In soil contamination, DNOC can be a potential threat to the microorganism community in the soil. Microbial ecological biodiversity is assumed to be the primary key to recovering soil microorganism communities. Soil microorganisms have the highest risk of being the target of using DNOC as an herbicide. It interferes with the material cycle and nutrient cycle in the soil. This condition is a fundamental problem because the composition of the soil microflora will determine the biological and chemical quality of the soil (Wolejko et al., 2020). The average allowable daily dose of DNOC is 3 mg/kg/day, and it includes toxic compounds with an LD50 value of 26-34 mg/kg in rats. The accumulation of DNOC in the human body is indicated to have the potential to harm the male reproductive system (US EPA, 2009). A study that conducted 54 mg/kg DNOC for 24 days on male rats showed a reduced testicular morphological effect and a decreased sperm quality at a dose of 20 mg/kg DNOC for 20 days, resulting in chromosomal aberration in male rats and significantly increasing abnormal sperm incidence in 15 mg/kg of DNOC dose (Takahashi et al., 2006). It occurs because DNOC inhibits cellular respiration and triggers DNA degradation (Aranha et al., 2007).

### CONCLUSIONS

Based on this study, it can be concluded that MIP-DNOC can be successfully synthesized using the bulk method. Optimum adsorption parameters for DNOC adsorption are achieved at pH 5 with a contact time of 30 min using the batch method. MIP can still adsorb an initial concentration of 600 mg/L DNOC at an adsorption capacity of 137 mg/g even though the efficiency of adsorption is significantly reduced.

The DNOC adsorption process is shown to adhere to the Sips isotherm model ( $n = 0.967$ ), and the adsorption rate follows pseudo-second-order adsorption kinetics. MIP-DNOC is relatively reusable even after three adsorption-desorption cycles using a mixture of methanol/acetic acid in a ratio of 3:1 as the eluent for desorption. The concentration of DNOC in tomato samples is 0.65 mg/kg, which is still within the minimum limit range for pesticide residues allowed by the government.

### ACKNOWLEDGMENTS

The authors are grateful to the Research and Technology of the Republic of Indonesia (Ristekdikti) (number 2427.1/D/KPT/2017 for financially supporting this research.

### REFERENCES

- Aboueilla, D.M., Fateen, S.E.K., Fouad, M.M.K. (2018). Multiscale modelling study of the adsorption of CO<sub>2</sub> using different capture materials, *Evergreen*, 5(1), 43-51.
- Aranha, M., Matos, A.R., Teresa, A., Vaz, V., Arrabac, D. (2007). Dinitro-o-cresol induces apoptosis-like cell death but not alternative oxidase expression in soybean cells. *Journal of Plant Physiology*. 164, 675–684.
- Arora, P.K., Srivastava, A., Singh, V.P. (2014) Bacterial degradation of nitrophenols and their derivatives. *Journal of Hazardous Materials*, 266, 42-59.
- Ashley, J., Shahbazi, M., Kant, K., Chidambara, V.A., Wolffa, A., Bang, D., Sun, Y. (2017). Molecularly imprinted polymers for sample preparation and biosensing in food analysis: Progress and perspectives. *Biosensors and Bioelectronics*, 91 (January), 606–615.
- Chen, F., Ba, S., Tang, W. (2015). Preparation and characterization of nonylphenol magnetic molecularly imprinted polymer. *Journal of The Chemical Society of Pakistan*, 37 (6), 1143-1152.
- Cheng, J., Ding, C., Li, X., Zhang, T., Wang, X. (2015). Rare earth element transfer from soil to navel orange pulp (*Citrus sinensis* Osbeck cv. Newhall) and the effects on internal fruit quality. *PLoS One*, 10(3), 1–15.
- Dwivedi, S.P., Maurya, M., Maurya, N.K., Srivastava, A.K., Sharma, S., Saxena A. (2020). Utilization of groundnut shell as reinforcement in development of aluminum-based composite to reduce environment pollution: A review. *Evergreen*, 7(1), 15-25.
- Ferreira, I., Fernandes, J.O., Cunha, S.C. (2012). Optimization and validation of a method based in a QuEChERS procedure and gas chromatography-mass spectrometry for the determination of multi-mycotoxins in popcorn. *Food Control*, 27(1), 188–193.

- Fu, X., Yang, Q., Zhou, Q., Lin, Q., Wang, C. (2015). Template-monomer interaction in molecular imprinting: Is the strongest the best? *Open Journal of Organic Polymer Materials*, 05(02), 58–68.
- Gao, N., Dong, J., Liu, M., Ning, B., Cheng, C., Guo, C., Zhou, C., Peng, Y., Bai, J., Gao, Z. (2012). Development of molecularly imprinted polymer films used for detection of profenofos based on a quartz crystal microbalance sensor. *Analyst Journal*, 137(5), 1252–1258.
- Hlihor, R., Olga, M., Rosca, M., Cozma, P. (2019). Modelling the behavior of pesticide residues in tomatoes and their associated long-term exposure risks. *Journal of Environmental Management*, 233, 523–529.
- Jeong, H. R., Lim, S. J., Cho, J. Y. (2012). Monitoring and risk assessment of pesticides in fresh omija (*Schizandra chinensis* Baillon) fruit and juice. *Food and Chemical Toxicology*, 50(2), 385–389.
- Krishnan, K.A., Suresh, S.S., Arya, S., Sreejalekshmi, K.G. (2015). Adsorptive removal of 2,4-dinitrophenol using active carbon: kinetic and equilibrium modeling at solid–liquid interface. *Desalination Water Treatment*, 54 (7), 1850–1861.
- Lezamiz, J. and Jönsson J.Å. (2007). Development of a simple hollow fibre supported liquid membrane extraction method to extract and preconcentrate dinitrophenols in environmental samples at ng L<sup>-1</sup> level by liquid chromatography. *Journal Chromatography A*, 1152(1–2), 226–233.
- Liu, S., Zheng, Z., Li, X. (2013). Advances in pesticide biosensors: Current status, challenges, and future perspectives. *Analytical and Bioanalytical Chemistry*, 405(1), 63–90.
- López-Lorente, A.I., Pena-Pereira, F., Pedersen-Bjergaard, S., Zuin, V.G., Ozkan, S.A., Psillakis, E. (2022). The ten principles of green sample preparation. *TrAC Trends in Analytical Chemistry*, 148, 116530.
- Mahmood, M.H., Sultan, M., Miyazaki, T. (2019). Study on water-vapor adsorption onto polymer and carbon-based adsorbents for air-conditioning application. *Evergreen*, 6(3), 215–224.
- Mehdinia, A., Ahmadifar, M., Aziz-Zanjani, M.O., Jabbari, A., Hashtroudi, M.S. (2012). Selective adsorption of 2,4-dinitrophenol on molecularly imprinted nanocomposites of mesoporous silica SBA-15/polyaniline. *Analyst Journal*, 137(18), 4368–4374.
- Pelfrene, A. F. (2000). Dinitro-ortho-cresol. Geneva (Switzerland) WHO.
- Putri, A.A.A., Hartini, S., Purwaningsih, R. (2021). Sustainable value stream mapping design to improve sustainability performance of animal feed production process. *Evergreen*, 8(1), 107–116.
- Rahman, M.M., Pal, A., Uddin, K., Thu, K., Saha, B.B. (2018). Statistical analysis of optimized isotherm model for Maxsorb III/ethanol and silica gel/water pairs. *Evergreen*, 5(4), 1–12.
- Rosmalina, R.T., Amran, M.B., Priatni, S. (2019). Preparation and characterization of dinitro-ortho-cresol molecularly imprinted polymer. *Proceeding of 2<sup>nd</sup> International Conference on Modern Research in Engineering, Technology, and Science*.
- Sakthiselvi, T., Paramasivam, M., Vasanthi, D., Bhuvanewari, K. (2020). Persistence, dietary and ecological risk assessment of indoxacarb residue in/on tomato and soil using GC – MS. *Food Chemistry*, 328 (March) 127–134.
- Salehi, B., Sharifi-Rad, R., Sharopov, F., Namiesnik, J., Roointan, A., Kamle, M., Kumar, P., Martins, N., Sharifi-Rad, J. (2019). Beneficial effects and potential risks of tomato consumption for human health: An overview. *Nutrition*, 62, 201–208.
- Samarth N. B., Kamble, V., Mahanwar, P.A., Rane, A.V., Abitha K.K. (2015). A historical perspective and the development of molecular imprinting polymer-a review. *Chemistry*, 1(4), 202–210 (2015).
- Singh, K.P., Kumar, A., Tyagi, S., Singh, R., Singh, P. (2014). Selective recognition of endosulfan pesticide in environmental matrix with molecularly imprinted polymer membrane," *Research Journal of Chemical Science*, 4(4), 63–70.
- Supramono, D., Lana, E.H., Setiadi, Nasikin, M. (2019). Effect of carrier gas flow rate on bio-oil yield and composition in corn cobs and polypropylene plastic slow co-pyrolysis," *Evergreen*, 6(2), 149–156.
- Takahashi, K.L., Takahashi, N., Hojo, H., Kuwahara, M., Aoyama, H., Teramoto, S. (2006). Pathogenetic transition in the morphology of abnormal sperm in the testes and the caput, corpus, and cauda epididymides of male rats after treatment with 4,6-dinitro-o-cresol. *Reproductive Toxicology*, 22(3), 501–507.
- Thi, H., Hai, N., Thu, H., Kadokami, K. (2021). Occurrence and risk assessment of herbicides and fungicides in atmospheric particulate matter in Hanoi, Vietnam. *Science of Total Environment*, 787, 147674.
- US Environmental Protection Agency (2009). Risk Assessment Guidance for Superfund Volume I: human health evaluation manual (part F, Supplemental Guidance for Inhalation Risk Assessment).
- US Environmental Protection Agency (EPA) (2014). Framework for human health risk assessment to inform decision making. EPA/100/R-

- 14/001.
- Wang, X., Jia, R., Song, Y., Wang, M., Zhao, Q., Sun, S. (2019). Determination of pesticides and their degradation products in water samples by solid-phase extraction coupled with liquid chromatography-mass spectrometry. *Microchemical Journal*, 149(June), 104013.
- Wang, Z., Ye, C., Li, J., Wang, H., Zhang, H. (2013). Comparison and evaluation of five types of imidazole-modified silica adsorbents for the removal of 2,4-dinitrophenol from water samples with the methyl group at different positions of imidazolium ring. *Journal of Hazardous Material*, 260, 955–966.
- Wojtko, E., Jabłońska-Trypuć, A., Wydro, U., Butarewicz, A., Łozowicka, B. (2020). Soil biological activity as an indicator of soil pollution with pesticides – A review. *Applied Soil Ecology*, 147, 103356.
- Yahya, N.Y., Chan, J.X., Ngadi, N. (2021). Biosorption of chromium (VI) ions using sustainable eggshell impregnated *Pandanus amaryllifolius roxb.* Biosorbent. *Evergreen*, 8(1), 146-155.
- Yusiasih, R., Pitoi, M.M., Endah, E.S., Ariyani, M., Koesmawati, T.A. (2021). Pyrethroid residues in Indonesian cocoa powder: Method development, analysis and risk assessment. *Food Control*, 119, 107466.